# Comparison of the Energetics of Desorption of Solution and Vapour Phase Deposited Analytes in Graphite Furnace Atomic Absorption Spectrometry

**Sean Lynch,* Ralph E. Sturgeon† and Van T. Luong**
*Division of Chemistry, National Research Council of Canada, Ottawa, Ontario K1A 0R9, Canada*
**David Littlejohn**
*Department of Pure and Applied Chemistry, University of Strathclyde, 295 Cathedral Street, Glasgow G1 1XL, UK*



The energetics of atomisation of Pb, Cu, Ag and Au in pyrolytic graphite coated, uncoated electrographite and glassy carbon tubes was studied following deposition of the analyte as a solution (primary site) and as an aerosol vapour (secondary site). Arrhenius activation energies ($E_a$) for Pb and Cu were independent of tube type and mode of analyte deposition. An apparent first-order rate of release occurs from all tube types and from both primary- and secondary-deposition sites, suggesting that both elements desorb from the surface as individual atoms. Values of $E_a$ for desorption of Ag and Au were independent of furnace tube type but dependent on the deposition mode, with fractional orders of desorption obtained throughout. Data for these elements suggest the formation of micro-droplets or caps (primary site) and islands (secondary site) with desorption occurring from the droplet surface or at the metal - graphite interface.

**Keywords:** *Graphite furnace; atomic absorption spectrometry; activation energy; desorption*

The shapes of transient atomic absorption (AA) signals developed with electrothermal atomisers have been shown, in many instances, to be determined by the rate of release of analyte from the substrate rather than by diffusive loss from the analytical volume.[1,2] Early studies by van den Broek and de Galan[3] pointed to the difficulty of modelling signal transients in tubular graphite furnaces, even after careful experimental separation of the supply and removal functions. Two reasons were suggested to account for this: (*i*) adsorption and re-desorption of vaporised analyte atoms produce a secondary supply of atoms, elongating the over-all supply function; and (*ii*) the supply function can only be approximately described in terms of a single first-order Arrhenius type rate constant, *i.e.*, experimentally derived activation energies ($E_a$) characterising analyte release may be valid only for a portion of the analyte atoms.

The shape of the supply function depends on the physicochemical properties of the graphite surface interacting with the analyte.[4] Specific analyte - substrate interactions have also been studied by Holcombe *et al.*,[5] where radially resolved spatial distributions of analyte vapour within the furnace have revealed the affinity of the vapour of some elements (*e.g.*, Cu) for clean graphite at high temperature; other elements (*e.g.*, Ag) display evidence of a more pronounced metal - metal interaction energy, as opposed to such strong metal - graphite interactions.

Paveri Fontana *et al.*[6,7] were the first to suggest that desorption of analyte from the furnace wall could be considered a pseudo-equilibrium process, where the vapour flux desorbed from the wall is equal to that subsequently adsorbed. Musil and Rubeska[8] developed a kinetic model for atomisation which incorporated rate constants for such re-deposition and re-desorption processes. Welz *et al.*[9] successfully extended this concept to a temporally and spatially non-isothermal furnace. These workers[9] attempted to quantify the $E_a$ values associated with the re-desorption of analyte atoms from these secondary desorption sites. Qualitatively evident from their study was the marked effect produced by a change in the $E_a$ value characterising re-desorption from secondary sites on the shape of a signal transient that had a fixed $E_a$ governing the initial release of atoms.

Accurate, quantitative information characterising the $E_a$ for the release of analyte atoms from secondary surface sites is lacking.[9,10] Such data should prove valuable in modelling transient AA signals, providing fundamental information on the energetics of carbon - metal atom interactions and an insight into the nature of analyte atomisation and the morphology of analyte distributions on the graphite surface.

The present study was undertaken to measure the energetics of desorption of both initial or primary analyte deposition from conventional solution sample residues and that characterising desorption of atoms from secondary sites arising from the deposition of analyte vapour on to the graphite tube wall. Comparison of these $E_a$ values and the corresponding orders of desorption[11] with respect to the mode of analyte deposition should prove useful in identifying likely condensed-phase precursors to free analyte vapour and provide insight into the topology of the condensed phase primary-desorption site.

Lead, Cu, Ag and Au were selected for study. Lead and Cu are reported to interact more strongly with graphite than Ag or Au; these last elements tend not to wet graphite, exhibit relatively weak metal - graphite interactions and lead to the formation of metal micro-droplets.[11,12] Primary and secondary analyte desorption energies from three types of furnace tubes, *i.e.*, pyrolytic graphite coated electrographite (PGC), uncoated electrographite (EG) and glassy carbon (GC) were compared.

## Experimental

### Apparatus

Atomic absorption measurements were made using a Perkin-Elmer Model HGA-2200 furnace (Perkin-Elmer, Norwalk, CT, USA) mounted on a Varian Techtron Model AA-5 spectrometer (Varian Techtron, Mulgrave, Victoria, Australia). Cathodeon (Cambridge, UK) (Pb, Cu and Au) and Varian (Ag) hollow-cathode lamps, operated at their recommended currents, served as line sources for the primary resonance wavelengths of the elements. Nominal spectral

* On leave from the University of Strathclyde.
† To whom correspondence should be addressed.
NRCC No. 31260.

bandpasses of 0.1 (Ag and Au), 0.2 (Cu) and 0.05 (Pb) nm were used.

Phototube voltage was digitised with 12-bit resolution using a DAS-8 eight-channel analogue to digital (A/D) card (MetraByte, Taunton, MA, USA) operated at 9 kHz. Data were collected with an IBM AT and manipulated with in-house software written in TURBO PASCAL version IV (Borland International, Scotts Valley, CA, USA). Signal intensity was corrected for furnace emission, absorbance - time profiles were calculated and the signals either subjected to fast Fourier filtering and/or a 25-point Savitzky - Golay moving average to give a smoothed signal. Activation energies, determined using the method proposed by Smets,[13] were obtained from a least-squares fit of the data.

Internal purge gas flow through the furnace was regulated using either one or other of two rotameters placed in parallel to cover the range 0–300 ml $min^{-1}$ and 0.6–15 l $min^{-1}$ of argon. External sheath gas was maintained at 1 l $min^{-1}$.

Temperature measurements were made with a Model 1100 automatic optical pyrometer (Ircon, Niles IL, USA). Blackbody radiation was imaged from the sample introduction hole. Output from the pyrometer was digitised and directly converted into temperature using calibration data which had been fitted to a ninth-order polynomial. Temperature - time data below about 850 °C (the lower limit measurable) were obtained by a least-squares linear extrapolation of the 1000–1200 °C region back to the start of the atomisation stage. Such procedures resulted in temperatures which were in good agreement with those attained at the end of the charring stage, as measured with a chromel - alumel thermocouple.

Unit emissivities, assumed for all tubes, should introduce negligible errors in the measured temperature.[14] This was confirmed for the GC tubes where no measurable temperature difference was recorded for the heating of a clean tube and following deposition of an amorphous graphite coating on the interior surface by the pyrolysis of methane.[15]

All temperature and signal intensity data were recorded simultaneously during each atomisation cycle.

Perkin-Elmer EG and PGC tubes were used. Glassy carbon tubes were obtained from Ringsdorff-Werke (Bonn, FRG) as were the PGC T-tubes, similar to those described by Slavin and Manning.[16] The T-tube side arm was 4 cm long with a 0.6 cm o.d. × 0.3 cm i.d. The sample dosing port in the left-hand contact ring was enlarged in order to accommodate the T-tube side arm.

Electrothermal vaporisation from wire probes was used in some instances to achieve a secondary deposit of analyte on the furnace walls. A typical probe consisted of two thick parallel wire posts or leads, 15 cm long, approximately 0.5 cm apart and bridged at one end by a thin wire filament. Probe heating was achieved using a Variac and a 125 VA transformer (Hammond Manf., Guelph, Ontario, Canada) in parallel with an a.c. ammeter. Various combinations of post and filament material (Cu, W and Au) were investigated.

## Reagents

Stock solutions of Pb, Cu, Au and Ag were prepared by dissolution of the high-purity metals (Spex Industries, Metuchen, NJ, USA) in dilute $HNO_3$ or aqua regia. Working standards of these elements were prepared by serial dilution with distilled, de-ionised water (DDW), unless otherwise indicated.

Argon and compressed air (Union Carbide, Mississauga, Ontario, Canada) were used as an inert gas and for oxygenation of the graphite tube surfaces, respectively.

## Procedure

### *Primary desorption*

Sample solutions were manually dispensed in 10-μl aliquots, unless otherwise stated. Furnace tube injection ports were enlarged to a size similar to that described below for secondary desorption in order to preserve consistency between the two sets of experiments. Samples were typically dried at 120 °C using a 5-s heating ramp with a 30-s hold time and charred at 500 °C using a 5-s ramp with a 60-s hold time. Atomisation or desorption temperatures were set at 2200 °C for Pb, Ag and Au and 2500 °C for Cu. Heating rates for this stage were 450 K $s^{-1}$ (Pb, Ag and Au) and 650 K $s^{-1}$ (Cu) using PGC and EG tubes and 350 K $s^{-1}$ for all elements using GC tubes. Such low heating rates were useful in isolating the source functions for vaporisation of these elements. Internal purge gas flow was maintained at 2300 ml $min^{-1}$ during the dry and char stages but increased to levels sufficient to ensure isolation of source functions[3] during the atomisation stage.

**Table 1.** Drying programmes for Au and Ag

| Element | Tube | Drying rate | Temperature °C Ramp | Hold | Time/s |
|---|---|---|---|---|---|
| Au* . . . . | PGC | Slow | 120 | 5 | 40 |
| | | Fast | 250 | 1 | 30 |
| | EG/GC | Slow | 80 | 5 | 120 |
| | | Fast | 120 | 5 | 30 |
| Ag† . . . . | PGC/EG | Slow | 3 × 60 | 15 | 90 |
| | | Fast | 150 | 1 | 10 |
| | GC | Slow | 80 | 20 | 100 |
| | | Fast | 500 | 5 | 10 |

* 10-μl sample; internal purge 100 ml $min^{-1}$.
† 2-μl sample; internal purge 250 ml $min^{-1}$.

Activation energies were derived from Smets plots of the absorbance - temperature data[13] and the order of desorption[11] inferred from the effect of mass on the source function characteristics.

The effect of the rate of drying of the solution on the results for Ag and Au was studied. Table 1 summarises the fast and slow drying programmes used.

### *Secondary desorption*

Vapour deposition of a secondary source of analyte on to the furnace tube walls was initially attempted using a graphite platform. A platform, dosed with a sample and dried outside of the furnace, was briefly inserted into the furnace to permit sample charring. Following its removal (through the open right-hand side end window) the furnace was subjected to a high-temperature cleaning cycle. The platform was then placed back into the furnace and analyte vapour transferred to the tube walls by heating the furnace to a temperature close to the appearance temperature of the element under study. Despite the use of an internal purge gas flow, or even the use of "curtained tubes"[17] in efforts to localise secondary deposition to the centre of the tube, the majority of the analyte was found by experiment (surface leaching studies) to be deposited on the cooler extremities of the tube. This precluded accurate use of Arrhenius plots with the result that this method of secondary-site deposition was abandoned.

Electrothermal vaporisation from the wire probe as a means of obtaining a secondary deposit was successful for Pb and Cu. The probe was mounted on a retort stand and introduced through a slot (approximately 4 × 8 mm) cut in the side of the graphite tube. The filament was heated for 10–30 s using a 1–10-A current. An internal purge gas flow-rate of 50 ml $min^{-1}$ was used throughout to limit analyte deposition to the central region. Following deposition, the probe was carefully removed from the furnace and the secondary deposit of analyte was desorbed using the atomisation conditions cited earlier for primary deposits except that in this instance no sample charring was used. The mass of analyte deposited was subsequently estimated through comparison of integrated

**Table 2.** Typical linear range of Arrhenius plots; PGC tube, $dT/dt$ = 450 K $s^{-1}$ (Pb, Au and Ag), 650 K $s^{-1}$ (Cu)

| Element | Deposition mode* | Flow-rate†/ ml $min^{-1}$ | Mass/ng | Peak temperature/K | Linear range/K |
|---|---|---|---|---|---|
| Pb . . . . | Primary | 150 | 5 | 1415 | 1210–1380 |
| | Secondary | 100 | 19 | 1365 | 1130–1305 |
| Cu . . . . | Primary | 40 | 0.8 | 1830 | 1340–1830 |
| | | 200 | 10 | 1620 | 1245–1500 |
| | Secondary | 50 | 1.1 | 1800 | 1320–1770 |
| | | 200 | 1.9 | 1750 | 1330–1750 |
| Au . . . . | Primary | 0 | 0.8 | 1525 | 1375–1530 |
| | | 100 | 1.0 | 1530 | 1355–1545 |
| | Secondary | 0 | 0.15 | 1370 | 1080–1375 |
| | | 100 | 0.39 | 1395 | 1115–1400 |
| Ag . . . . | Primary | 250 | 1.0 | 1320 | 1215–1330 |
| | Secondary | 250 | 0.55 | 1165 | 1000–1165 |

* Primary, solution deposition; and secondary, vapour deposition.
† Internal Ar purge gas.

**Table 3.** Desorption energetics of lead; internal Ar purge, 100 ml $min^{-1}$; heating rate, 450 K $s^{-1}$ (PGC and EG), 350 K $s^{-1}$ (GC)

| Tube | Deposition mode* | Mass/ng | $E_a$†/kcal $mol^{-1}$ |
|---|---|---|---|
| PGC . . . . | Primary | 4–10 | 52 ± 5 (11) |
| | Secondary, P | 8.5–23 | 52 ± 6 (6) |
| | T | 1.0–3.5 | 47 ± 5 (9) |
| | $O_2$ | | 54 ± 4 (3) |
| EG . . . . . | Primary | 3.0–20 | 57 ± 6 (13) |
| | Secondary, P | 3.0–21 | 53 ± 7 (13) |
| | $O_2$ | | 51 ± 2 (3) |
| GC . . . . . | Primary | 2.0–10 | 43 ± 3 (20) |
| | Secondary | 0.7–9 | 47 ± 5 (14) |

* P, Probe deposition; T, T-tube secondary site vapour deposition; and $O_2$, oxidised surface.
† Mean and standard deviation of ($n$) replicate determinations.

absorbance with that recorded for known amounts of primary deposits. Surface leaching experiments confirmed that the majority of the deposit was located within the central 7 mm of tube length.

A study of the effect of tube wall temperature during secondary deposition on the energetics of desorption of these species was also implemented. Additionally, the influence of an oxygenated surface (achieved by heating the tubes to 900 °C for 2 min in a 1 l $min^{-1}$ stream of compressed air) on the desorption of secondary site Pb from the PGC and EG tubes was studied.

Vapour deposition of Pb was achieved by heating a filament of Cu wire (diameter 0.2 mm) on to which Pb metal had been melted. The Cu filament was supported by 1-mm diameter Cu posts. For Cu, a probe with a W filament (diameter 0.2 mm) supported on Cu posts was heated, causing localised heating of the Cu posts, which resulted in the vaporisation of sufficient Cu.

Irregular and imprecise signals were obtained for the atomisation of Au introduced as secondary deposits using the heated wire probe. Various combinations of post material (Au or Cu), filament (Au or W) and analyte source (Au wire, electrodeposited Au film or dried and thermally reduced solution residue on W wire) were used but the problems persisted and this approach was abandoned. For Ag, satisfactory signals for secondary desorption could be obtained when samples were vapour deposited from a heated W filament on to which Ag had been electrodeposited. However, this study was not pursued.

Secondary deposits of all analytes could also be achieved using a T-tube configuration, where a reservoir or collection tube was mounted on the end of the side arm. The injection port of the furnace into which the analytes were vapour deposited (the collection tube) was enlarged to 5 mm in diameter in order to achieve close contact with the tapered end of the T-tube side arm.

The T-tube was initially inserted into the furnace workhead. Removal of the right-hand window assembly permitted 2–20-µl volumes of analyte solutions (2.5–500-ng masses) to be manually pipetted on to the centre of the tube. The window was replaced, the sample was then dried (120 °C; 15-s ramp, 40-s hold), charred (500 °C for Ag, Cu and Pb; 850 °C for Au; 10-s ramp, 60-s hold) and cooled to room temperature while maintaining a flow-rate of 150–200 ml $min^{-1}$ of internal purge gas. The collection tube (which had been previously cleaned using several high temperature cycles) was then placed on the top of the T-tube stem, the sample vaporised by heating the T-tube (2200 °C for Pb, Ag and Au; 2500 °C for Cu; 5-s ramp, 1-s hold) and the analyte vapour transported up the stem and into the collection tube where a fraction of it was trapped. The flow-rate of the internal purge gas (150 ml $min^{-1}$ for Ag; 200 ml $min^{-1}$ for Au, Cu and Pb) was sufficient to ensure that the atmosphere in the collection tube was similar to that for atomisation performed in a normal graphite furnace under gas flow conditions. Following this short atomisation step, the collection tube was quickly removed using Pt-tipped tongs and placed in a clean receptacle. The T-tube was then removed, the collection tube fitted into the furnace workhead and the secondary sample vaporised using the heating programme given for the primary-site desorption, with the exception that the sample was not charred.

Surface leaching studies of the secondary deposits confirmed that vapour deposition was confined to the centre of the collection tube..

Transmission electron micrographs of the secondary analyte deposits of Pb, Ag and Cu were attempted using a Philips (Cambridge, UK) EM 430 microscope operated at a 250-kV accelerating voltage. Thin films of vapour-deposited carbon were transferred to graphite electron microscope grids (3 mm diameter). The grids were then placed in a PGC tube and a secondary deposit (0.5–5 ng) was transferred on to the thin carbon film using the wire-probe technique. Unfortunately, only Pb deposits were successfully investigated in this manner.

## Results and Discussion

Table 2 summarises the temperature ranges over which linear segments of Arrhenius plots were established for each element and mode of deposition in a PGC tube. For comparative purposes, the temperature at the maximum of the source function is also given. In most instances, data from nearly the total rising edge of the transient could be used for calculation of the resultant $E_a$ value.

It can also be seen that relatively low internal purge gas flow-rates were required for isolation of the source function, this being a consequence of both the low rate of heating of the furnace during the desorption (atomisation) step and the enlarged sample injection port which gave rise to enhanced rates of diffusive loss of analyte vapour. Results presented for

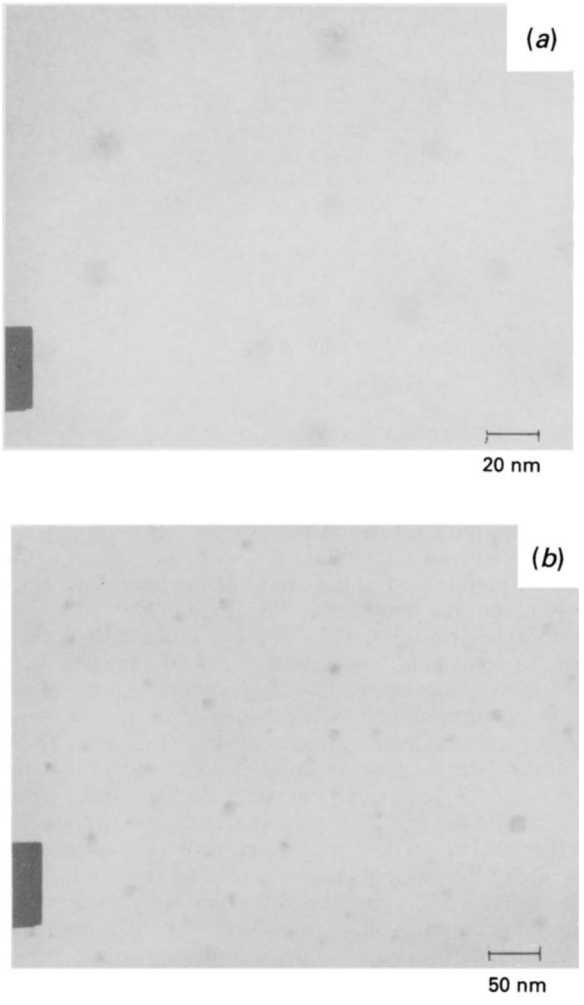


**Fig. 1.** Transmission electron micrograph (bright field images) of secondary-site (vapour deposited) Pb obtained with heated probe. Substrate is amorphous carbon film; estimated total Pb load, 5 ng. (*a*) 311 000 × magnification; and (*b*) 132 500 × magnification

the PGC tube in Table 2 are also typical of those obtained in the EG and GC tubes.

For ease of presentation, results for each analyte will be dealt with individually in the subsequent discussion.

## Lead

Table 3 summarises the measured primary- and secondary-desorption energies for lead calculated for all three tubes. Both the heated probe and T-tube were used to obtain secondary deposits via vapour deposition. Activation energies are essentially indistinguishable for all three tube types and for both primary- and secondary-desorption sites. Additionally, $E_a$ values appear to be independent of mass desorbed, within the range (0.7–23 ng) studied. The aim of vapour deposition experiments using wire probes and T-tubes was to achieve a secondary deposit of highly dispersed analyte, present as isolated adatoms on the surface, if possible, prior to desorption. Electron micrographs, shown in Fig. 1, illustrate the dispersion of Pb over the surface of a graphite film, obtained through the vapour deposition of approximately 5 ng of Pb using the wire-probe method. Evidence of a highly dispersed secondary deposit containing islands of Pb particles (confirmed by X-ray fluorescence) having an average diameter of 4.5 nm is clear. If the particles are spherical, they contain about 1500 atoms of Pb. If the images represent two-dimensional (2-D) islands, they contain about 160 atoms of Pb. Primary deposition of Pb from aqueous solution could also

**Table 4.** Effect of tube-wall temperature during vapour deposition on secondary-desorption energy of lead using heated-probe deposition on to tube wall; mean and standard deviation of (*n*) replicate determinations

| Wall temperature/K | Activation energy/kcal mol$^{-1}$ | | |
|---|---|---|---|
| | PGC | EG | GC |
| 300 | 52 ± 6 (6) | 53 ± 7 (13) | 43 ± 3 (20) |
| 710 | 51 ± 6 (6) | 55 ± 7 (3) | — |
| 780 | 46 ± 1 (3) | — | 59 (2) |
| 900 | 53 ± 8 (3) | 56 ± 6 (3) | 53 ± 12 (4) |
| 970 | — | 62 ± 5 (3) | — |

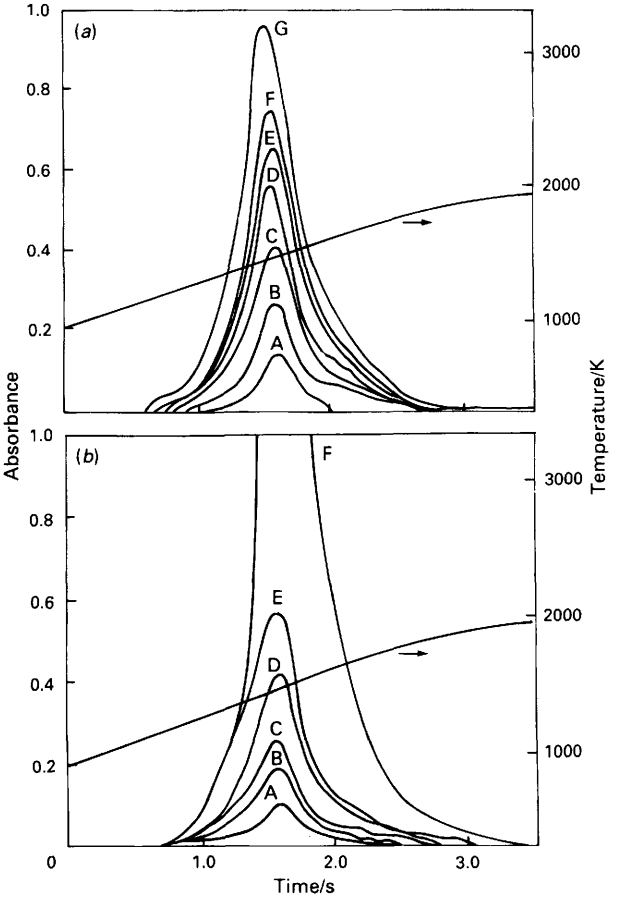


**Fig. 2.** Source functions for desorption of Pb from a glassy carbon surface. Diagonal lines show the measured tube temperatures. (*a*) Primary-site desorption for initial masses of: A, 1.0; B, 2.5; C, 3.5; D, 5.0; E, 6.0; F, 7.0; and G, 10.0 of ng Pb. (*b*) Secondary-site desorption of: A, 0.7; B, 1.7; C, 2.5; D, 4.0; E, 5.6; and F, 13.0 ng of Pb

result in a similar dispersion. The difficulty with drawing any conclusions from such evidence is that room-temperature morphology may not necessarily reflect that which exists at the moment (temperature) of rapid surface desorption because potential surface mobility may lead to either aggregation or further dispersion. Additionally, the physical character of the amorphous carbon film used for this illustration is substantially different from the pyrolytic graphite surface of the furnace tubes. Thus, direct comparison may not be practical.

The influence of surface dispersion on the $E_a$ values characterising desorption of secondary deposits was examined by observing the effect of tube-wall temperature during deposition on the resultant $E_a$ values. Data for Pb are summarised in Table 4, revealing no effect of deposition temperature, despite these values being within 150 K of the appearance temperature of the metal.

Activation energies summarised in Tables 3 and 4 averaged 49 ± 6 ($n$ = 44) for primary desorption and 49 ± 6 ($n$ = 42)

**Table 5.** Desorption energetics of copper

| Tube | Deposition mode* | Mass/ng | $E_a$†/kcal mol$^{-1}$ |
|---|---|---|---|
| PGC . . . . | Primary | 0.2–1.0 | 37 ± 3 (16) |
| | Secondary, P | 0.15–1.8 | 37 ± 2 (8) |
| | T | 0.5–5.5 | 42 ± 5 (13) |
| EG . . . . . | Primary | 0.5–3.5 | 31 ± 5 (19) |
| | Secondary | 0.7–2.4 | 27 ± 4 (7) |
| GC . . . . . | Primary | 0.5–3.5 | 35 ± 3 (9) |
| | Secondary | 0.15–2.5 | 30 ± 3 (8) |

* P, Heated probe deposition; and T, T-tube deposition.
† Mean and standard deviation of ($n$) replicate determinations.

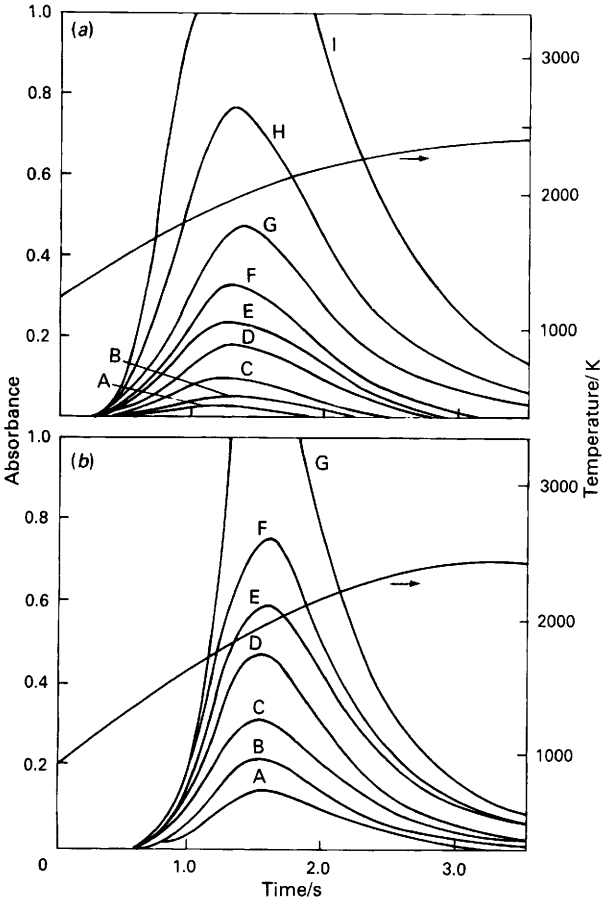


**Fig. 3.** Source function for desorption of Cu from EG (uncoated) tube surface. Diagonal lines are measured tube temperature. (*a*) Primary-site desorption for initial masses of: A, 0.5; B, 1.0; C, 2.0; D, 3.5; E, 5.0; F, 7.5; G, 10; H, 20; and I, 50 ng of Cu. (*b*) Secondary-site desorption of: A, 2.6; B, 4.3; C, 6.7; D, 9.8; E, 13; F, 16; and G, 26 ng of Cu

kcal mol$^{-1}$ for secondary desorption for all tubes ($n$ refers to the total number of measurements made for all tubes). These values are in good agreement with the thermodynamic heat of vaporisation ($\Delta H_{vap}$) of bulk Pb metal (48.5 kcal mol$^{-1}$ at 1000 K). This fact initially implicates bulk vaporisation from the reduced metal as the release mechanism; however, other observations are contrary to this suggestion.

Fig. 2 illustrates the effect of analyte mass on the absorbance - time profiles for desorption of both primary and secondary deposits of Pb from the surface of GC tubes. Identical peak temperatures (1415 ± 15 K) are obtained as the initial amount of analyte increases whereas an early shift occurs in the appearance temperature. Data shown for GC tubes in Fig. 2 are representative of similar occurrences with PGC and EG tubes. These observations are characteristic of an apparent first-order surface desorption[11] and indicative of release of Pb from a monolayer film or a field of highly

**Table 6.** Effect of tube-wall temperature during vapour deposition on the secondary-desorption energy of copper; heated-probe deposition on to tube wall; mean and standard deviation of ($n$) replicate determinations

| Wall temperature/K | Activation energy/kcal mol$^{-1}$ PGC | EG | GC |
|---|---|---|---|
| 300 | 37 ± 2 (8) | 27 ± 4 (7) | 30 ± 3 (8) |
| 710 | 37 ± 2 (3) | — | 35 ± 1 (3) |
| 900 | 35 ± 2 (3) | 27 ± 4 (3) | 33 ± 2 (4) |
| 970 | 37 ± 2 (3) | — | 37 ± 1 (3) |
| 1050 | — | — | 50 (2) |
| 1130 | 41 (2) | 27 ± 1 (4) | 46 ± 5 (6) |

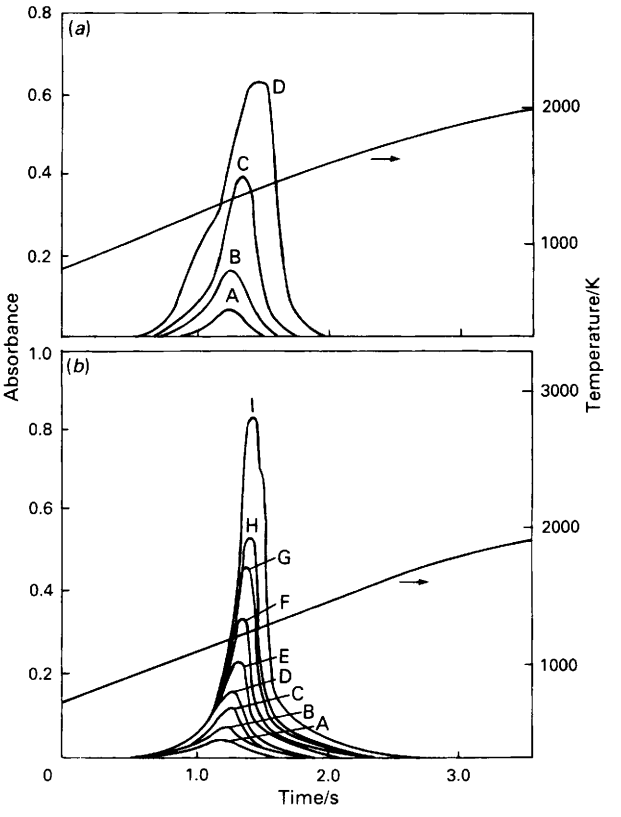


**Fig. 4.** Source functions for desorption of Ag from a PGC (coated) tube surface. Diagonal lines are measured tube temperature. (*a*) Primary-site desorption of: A, 0.10; B, 0.30; C, 1.0; and D, 2.0 ng of Ag. (*b*) Secondary-site desorption of: A, 0.10; B, 0.20; C, 0.35; D, 0.40; E, 0.45; F, 0.50; G, 0.70; H, 0.80; and I, 1.25 ng of Ag

dispersed atoms exhibiting significant metal - graphite interaction energy.

Agreement between $\Delta H_{vap}$ for bulk Pb metal and the $E_a$ values cited here is thus probably coincidental as bulk vaporisation of particles would lead to desorption orders of almost zero. The close correspondence in the signal characteristics for desorption from both primary and secondary sites argues that conventional solution deposition gives rise to a highly dispersed residue, possibly as a result of ion exchange with active sites on the graphite surface[17] or that, at or near the appearance temperature, surface mobility is such that the primary deposit becomes highly dispersed.

Earlier studies in this laboratory[18] reported an $E_a$ for the release of Pb from PGC tubes of about 90 kcal mol$^{-1}$, a value which appeared to correlate with the enthalpy change for the condensed-phase dissociation of PbO to yield $Pb_{(g)}$ and $O_2$. Samples had been prepared in 1% v/v $HNO_3$. In this study, preparation of working standards in 3.5% v/v $HNO_3$ gave $E_a$ values of 81 ± 11 kcal mol$^{-1}$ ($n$ = 8), increasing to 114 ± 25

**Table 7.** Desorption energetics of Ag; internal Ar purge, 250 ml min$^{-1}$; heating rate, 450 K s$^{-1}$

| | | Primary desorption | | | Secondary desorption† | |
|---|---|---|---|---|---|---|
| Tube | | Mass/ng | Drying rate* | $E_a$/kcal mol$^{-1}$ | Mass/ng | $E_a$/kcal mol$^{-1}$ |
| PGC | | 0.1–2 | Slow | 65 ± 7 (16) | 0.2–0.5 | 37 ± 4 (21) |
| | | 0.1–0.5 | Fast | 37 ± 2 (12) | | |
| EG | | 0.1–2 | Slow | 72 ± 7 (28) | 0.2–1.0 | 29 ± 4 (20) |
| | | | Fast | 72 ± 7 (8) | | |
| GC | | 0.1–4 | Slow | 70 ± 6 (31) | 0.1–0.4 | 37 ± 5 (17) |
| | | | Fast | 40 ± 4 (3) | | |

* Slow, 60 °C, 15-s ramp, 90-s hold repeated three times; fast, 150 °C, 1-s ramp, 10-s hold.
† T-tube, secondary site vapour deposition; mean and standard deviation of ($n$) replicate determinations.



kcal mol$^{-1}$ ($n$ = 8) as the $HNO_3$ content increased to 10% v/v. Late signal shifting was observed, as compared with those AA signals from DDW solutions. These $E_a$ values are significantly different from the 49 ± 6 kcal mol$^{-1}$ obtained with working standards prepared in DDW only and reflect a change in the rate-determining step for the release of $Pb_{(g)}$. Nitration of the tube surface may lead to intercalation of the analyte into the graphite substrate resulting in a correspondingly more difficult release mechanism.

Oxygenation of the heated tube surface at 900 °C using air as the internal purge gas has no significant effect on the energetics of Pb desorption from secondary deposits (Table 3). This is in agreement with the results of earlier studies on the effect of oxygen on AA signal transients.[19] Whereas no change in the desorption energy is noted following surface oxidation, late shifted AA signals arise due to secondary gas phase interactions involving $O_2$, CO and $CO_2$ equilibria with the gaseous analyte. This effect is absent when desorption from an oxygenated surface is conducted in vacuum.[20] It is believed that intimate contact of the analyte with the graphite takes place via chemisorbed species and that direct metal - graphite interaction is unlikely because strongly chemisorbed species are normally present.[21] Thus, in both instances, interaction of Pb with surface oxides is most likely and no effect on $E_a$ is to be expected, regardless of deliberate prior surface oxidation.

## Copper

Data for Cu are summarised in Table 5. Activation energies are identical for both primary- and secondary-release sites and in good agreement with primary values reported by Holcombe *et al.*,[11,22] *i.e.*, 29 ± 3 kcal mol$^{-1}$. Both the mode of secondary deposition and the nature of the graphite surface do not appear to play any significant role in governing the release energetics.

An apparent first-order rate of release was observed for desorption both from primary and secondary sites. Fig. 3 illustrates these typical signal characteristics, evident for all three tube types studied, *i.e.*, a shift to earlier appearance temperatures while peak temperatures remain constant (1640 ± 15 K for PGC, 1900 ± 20 K for EG and 1920 ± 20 K for GC) as local surface coverage (analyte mass) increases. The over-all average $E_a$ values, *i.e.*, 35 ± 4 kcal mol$^{-1}$ ($n$ = 44) for primary-solution deposition and 35 ± 7 kcal mol$^{-1}$ ($n$ = 36) for secondary-vapour deposition, differ significantly from the bulk heat of vaporisation of Cu ($\Delta H_{vap}$ = 84.6 kcal mol$^{-1}$ at 1250 K) and probably represent the $E_a$ for desorption of dispersed Cu atoms, a conclusion which is consistent with a first-order process. Good agreement between the primary- and secondary-desorption energies requires that primary-solution deposits of Cu become highly dispersed over the graphite surface prior to significant desorption. Evidence for this has recently been reported by Wang *et al.*[23]

Table 6 presents data illustrating the effect of the temperature of the tube wall during secondary-site deposition on the $E_a$ associated with desorption of these species. For release from EG and PGC surfaces there is no effect. However, it appears that $E_a$ may increase on GC surfaces as the deposition temperature increases. No explanation can be offered for this except for possible increased surface mobility at higher temperature favouring agglomeration of atoms and, hence, an $E_a$ reflecting increased Cu - Cu interactions. Unfortunately, this hypothesis was not verified by looking for an accompanying change in the desorption order (to <1) following high-temperature deposition. The unique character of GC in this respect may arise because of the low porosity and few surface active sites on this material as compared with PG and EG. These observations may find a parallel with those of Arthur and Cho[24] in their study of single-crystal graphite. As the adsorbate - substrate interaction energy diminishes (fewer active sites on the surface) the deposited layer tends to form two- and three-dimensional crystallites. Alternatively, increased surface mobility and/or increased desorption - re-desorption cycles with higher temperature may re-distribute a greater fraction of the deposit to the cooler ends of the tube, thereby resulting in an "apparent" increase in the measured $E_a$ (because of inaccurate desorption temperatures) with no change in the order of desorption.

As sample mass, *i.e.*, surface coverage, was increased beyond 2 ng, $E_a$ values for both primary and secondary desorption increased to the 45–50 kcal mol$^{-1}$ range, suggesting that an alternative process competes as the rate-limiting step and Cu - Cu interactions possibly become more intense. Arthur and Cho[24] have shown that, as multilayer coverage is approached, the $E_a$ for the vacuum desorption of Cu from graphite approaches that of the $\Delta H_{vap}$ of bulk Cu. Such interactions, however, are not of current interest to processes in the graphite furnace because the analyte mass is beyond the analytical range used.

## Silver

Temporally and spatially resolved absorbance profiles for Ag have indicated a nearly uniform atom distribution over the cross-section of the furnace throughout the entire atomisation cycle,[5] pointing to weak Ag - graphite interactions. The existence of Ag micro-droplets has also been postulated.[1]

Table 7 presents results for the $E_a$ values obtained for desorption of both primary and secondary deposits of Ag. In contrast to Pb and Cu, $E_a$ values for Ag are dependent on the mode of analyte deposition. Primary-solution deposits which are dried very slowly (*cf.* Table 1) yield $E_a$ values which approach the enthalpy of vaporisation of bulk Ag, *i.e.*, 72 kcal mol$^{-1}$ at 1000 K. The average $E_a$ for all tubes for slow drying of solution deposits is 70 ± 6 kcal mol$^{-1}$ ($n$ = 75). This observation is consistent with the possible existence of micro-droplets on the surface prior to desorption.

Fig. 4 presents the absorbance - time profiles for the desorption of primary Ag from PGC surfaces. A fractional order of release, possibly $\frac{2}{3}$,[11] is evident from the shifts in both appearance and peak temperature as the analyte mass increases, again indicative of the desorption of Ag from micro-droplets on the surface. These observations are in agreement with those of Holcombe[12] who obtained an $E_a$ of 54 ± 6 kcal mol$^{-1}$ and a $\frac{2}{3}$-order of release for Ag from primary-solution deposits which had been dried very slowly.

Slow evaporation of solvent evidently enhances the growth or nucleation of Ag particles. Rapid drying of aqueous solutions in PGC and EG tubes resulted in a signficantly lower $E_a$ for the release of Ag, presumably as a result of increased dispersion of finer particles over the tube surface and altered metal - metal or metal - graphite interactions. The over-all shapes of such signals were less reproducible than their slow dried counterparts but appeared to result in an order of desorption closer to unity, consistent with the above. Holcombe[12] also obtained lower desorption energies for the primary release of Ag when the solvent evaporation rate was rapid, dropping from 54 ± 6 to 28 ± 1 kcal mol$^{-1}$, consistent with the dispersion of fine particles.

Rapid drying of solutions in EG tubes failed to produce a change in the measured desorption energy. With the extended surface area, porosity and larger number of active surface sites on to which ion-exchange deposition reactions may take place,[17] a highly dispersed deposit would be expected in EG tubes regardless of solvent evaporation rate. Contrary to the above, "large" particle formation appears to be favoured in both instances, eluding a rational explanation based on this simple model. Release energies characterising desorption of Ag from primary sites arising from rapid solvent evaporation in PGC and GC tubes are in good agreement with $E_a$ values for desorption of Ag from secondary sites. Overall, an average value of 38 ± 3 kcal mol$^{-1}$ ($n$ = 15) was obtained, suggesting that the topology of the Ag particles produced through vapour deposition is similar to that arising from a fast solvent evaporation rate. Fig. 4(*b*) indicates that, despite attempts to produce a highly dispersed field of Ag atoms on the surface using vapour deposition techniques, a desorption order significantly <1, possibly $\frac{1}{3}$, results.[11] A fractional order of desorption from secondary sites was evident for all three tube types. Although large absorption signals could be recorded in the heated T-tube during the vapour deposition process, indicating that a significant fraction of metal was in the vapour rather than aerosol form, analyte aggregation occurred on the surface of the receiver tube. All steps taken to minimise this were ineffective, including transfer of the lowest possible mass of analyte, short atomisation times to limit heating of the receiver tube surface and large gas transfer flow-rates (10 l min$^{-1}$) to limit deposition to the site of first impaction with the surface rather than permitting multiple collisions with preferential adsorption at and growth of an existing nucleation site. The fractional order of release is indicative of the presence of hemispherical caps or island structures on the surface. Such a surface topology may be because of significant adatom mobility on the graphite surface prior to the appearance temperature of Ag, resulting in the aggregation of highly dispersed atoms during the temperature ramp. Similar (vacuum evaporation) surface decoration techniques have also reported existence of a highly dispersed field of Ag micro-droplets on graphite.[21]

Table 8 illustrates the effect of mass on the $E_a$ of desorption of secondary deposits of Ag from PGC tubes. Beyond about 0.5 ng, the $E_a$ increases to about 60 kcal mol$^{-1}$, approaching the $\Delta H_{vap}$ for bulk Ag and the $E_a$ for desorption of primary site Ag using a slow solvent evaporation step. Evidently, an increase in the mass of analyte vapour deposited results in the further growth of existing particles as opposed to an increase in the number of particles.

**Table 8.** Effect of mass on energetics of desorption of secondary deposits of Ag; T-tube; mean and standard deviation of ($n$) replicate determinations

| Mass/ng | $E_a$/kcal mol$^{-1}$ |
|---|---|
| 0.2 | 36 ± 2 (4) |
| 0.3 | 36 ± 3 (4) |
| 0.35 | 39 ± 6 (3) |
| 0.4 | 36 ± 3 (4) |
| 0.45 | 39 (1) |
| 0.5 | 39 ± 5 (5) |
| 0.55 | 42 (2) |
| 0.7 | 50 (1) |
| 0.75 | 48 (1) |
| 0.8 | 54 (1) |
| 0.85 | 50 (1) |
| 1.1 | 56 (1) |
| 1.3 | 58 (1) |

## Gold

Results for primary desorption of Au have previously been reported.[11] Activation energies (71 kcal mol$^{-1}$) approaching the $\Delta H_{vap}$ were obtained and a $\frac{1}{3}$-order of release from the metal graphite interface of hemispherical structures was implicated.

Table 9 summarises $E_a$ data for both primary- and secondary-site desorption of Au. As for Ag, the rate of solvent evaporation had an effect on the results. Slow drying presumably fostered the development of bulk crystallites and the over-all primary site $E_a$ of 83 ± 5 kcal mol$^{-1}$ ($n$ = 10) approaches the $\Delta H_{vap}$ of Au ($\Delta H_{1250K}$ = 93 kcal mol$^{-1}$). This figure is in good agreement with data reported earlier from this laboratory.[18] Desorption energies were independent of sample mass over a broad range of "nominal surface coverage." "Local" coverages, where desorption is taking place, may, in fact, be multi-layered, thus accounting for the absence of change with increasing amount of analyte. However, no clear trend developed with respect to the effect of the rate of evaporation of the solution on the $E_a$ in all three tubes.

**Table 9.** Desorption energetics of Au; internal Ar purge at 100 ml min$^{-1}$; heating rate, 450 K s$^{-1}$; mean and standard deviation of ($n$) replicate determinations

| | Primary desorption | | | Secondary desorption† | |
|---|---|---|---|---|---|
| Tube | Mass/ng | Drying rate* | $E_a$/kcal mol$^{-1}$ | Mass/ng | $E_a$/kcal mol$^{-1}$ |
| PGC . . . . . | 0.2–5 | Slow | 84 ± 5 (44) | 0.05–0.2 | 48 ± 5 (35) |
| | | Fast | 40 | | |
| EG . . . . . | 0.2–2 | Slow | 80 ± 6 (32) | 0.2–0.5 | 45 ± 2 (9) |
| | | Fast | 67 | | |
| GC . . . . . | 0.1–2 | Slow | 85 ± 8 (25) | 0.2–0.5 | 42 ± 4 (8) |
| | | Fast | 73 | | |

* Slow, 60 °C, 15-s ramp, 90-s hold, repeated three times; and fast, 150 °C, 1-s ramp, 10-s hold.
† T-tube, secondary site vapour deposition.

**Table 10.** Effect of mass on the energetics of Au desorption from secondary sites; T-tube secondary site vapour deposition; mean and standard deviation of ($n$) replicate determinations

| PGC | | EG | | GC | |
|---|---|---|---|---|---|
| Mass/ng | $E_a$/kcal mol$^{-1}$ | Mass/ng | $E_a$/kcal mol$^{-1}$ | Mass/ng | $E_a$/kcal mol$^{-1}$ |
| 0.05 | 44 ± 5 (7) | 0.2 | 49 (1) | 0.25 | 44 (2) |
| 0.1 | 37 (2) | 0.25 | 47 ± 2 (3) | 0.3 | 44 ± 3 (4) |
| 0.15 | 44 ± 4 (4) | 0.3 | 44 (2) | 0.4 | 36 (2) |
| 0.2 | 45 (2) | 0.4 | 44 (2) | 0.6 | 51 ± 1 (4) |
| 0.25 | 49 ± 1 (3) | 0.5 | 44 (1) | 0.7 | 49 (1) |
| 0.3 | 54 (2) | 0.7 | 48 (1) | 1.0 | 57 (2) |
| 0.35 | 52 ± 1 (4) | 0.8 | 48 (1) | 1.2 | 51 (1) |
| 0.4 | 53 (1) | 1.5 | 49 (1) | 2.5 | 61 (2) |
| 0.5 | 51 ± 4 (3) | 1.7 | 54 (1) | | |
| 0.6 | 67 (1) | 2.5 | 49 (1) | | |
| | | 4.0 | 59 (1) | | |
| | | 5.0 | 56 (1) | | |

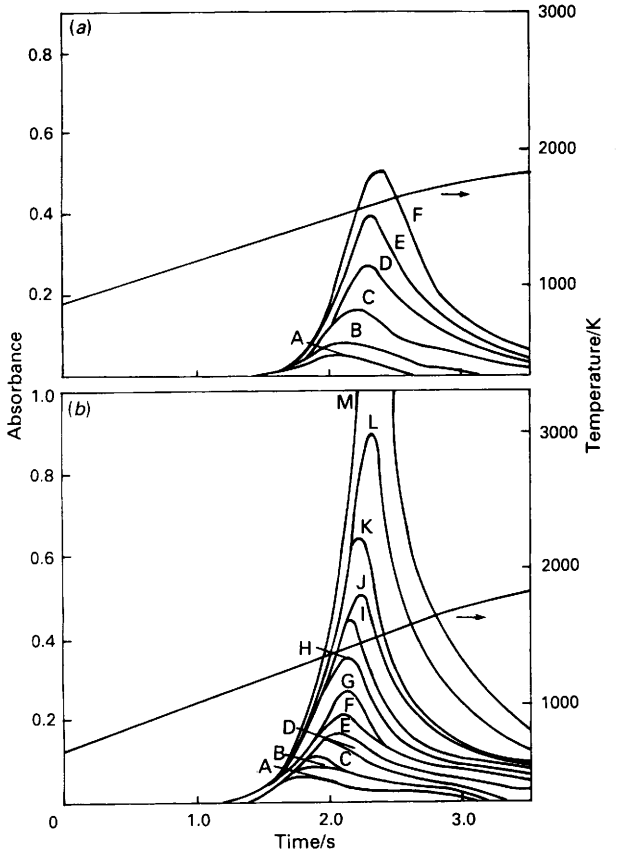


**Fig. 5.** Source function for desorption of Au from a PGC (coated) tube surface. Diagonal lines are measured tube temperature. (*a*) Primary-site desorption of: A, 0.10; B, 0.20; C, 0.40; D, 0.60; E, 0.80; and F, 1.0 ng of Au. (*b*) Secondary-site desorption of: A, 0.05; B, 0.07; C, 0.10; D, 0.13; E, 0.15; F, 0.18; G, 0.21; H, 0.25; I, 0.30; J, 0.34; K, 0.40; L, 0.50; and M, 0.75 ng of Au

Fig. 5 shows absorbance - time profiles of the source functions isolated for Au in the PGC tube. As the mass of analyte increases, the peak temperature increases whereas the appearance temperature shifts to slightly lower values, indicative of an apparent $\frac{1}{3}$-order of release. This is consistent with earlier results of McNally and Holcombe,[11] suggesting vaporisation of Au atoms from caps on the surface, hence the measured $E_a$ should not be correlated with the $\Delta H_{vap}$ (thermodynamic) but rather the specific release energy for Au atoms at the metal - graphite interface of the cap or from its surface.

Activation energies characterising desorption of Au from vapour deposited secondary sites (Table 9) are significantly lower than their primary site solution deposited counterparts, averaging 47 ± 2 kcal mol$^{-1}$ ($n$ = 52) for the three tubes studied. Fig. 5 presents data which suggest that the apparent order of release of Au from such secondary sites lies between $\frac{1}{3}$ and $\frac{2}{3}$,[11] possibly $\frac{1}{2}$, thus reflecting the presence of 2-D islands on the graphite surface at the temperature of significant desorption.

As the mass of Au vapour deposited on to secondary sites is increased, the desorption energy increases to approximately 66 kcal mol$^{-1}$, as illustrated by the data in Table 10. Vacuum deposition of vapour phase Au atoms also showed an increase in desorption energy from 51.8 to 73.5 kcal mol$^{-1}$ as the surface coverage was increased.[24] A $\frac{1}{3}$-order of desorption for sub-monolayer coverage was reported.[24] This leads to the conclusion that the morphology of secondary-site deposits changes above a critical mass load, possibly from a dispersion of 2-D islands to one of micro-droplets or caps with a concurrent change in the $E_a$ for desorption. Thus, the $E_a$ values presented in Table 9 characterising the release of Au atoms from secondary sites obviously do not reflect the energy of desorption of Au atoms from graphite but are approaching this value at low mass coverages (*i.e.*, <0.2 ng) and possibly serve as a measure of the upper limit.

The temperature of the graphite tube surface at which secondary site analyte deposition occurred had no effect on the resultant primary site $E_a$ results below 870 K. When Au was vapour deposited on to a tube surface whose temperature was 970 K, the resultant $E_a$ characterising desorption increased from 44 to 70 kcal mol$^{-1}$, suggesting that increased surface mobility at elevated temperatures may lead, within the 30-s time frame of the experiment, to island agglomeration and a corresponding increase in desorption energy characteristic of micro-droplets or caps.

## Conclusions

Heterogeneous analyte atom - graphite wall interactions are clearly of importance in determining the characteristics of sample atomisation.[1,4,9] Use of a pseudo-equilibrium approach to describe analyte release from the tube surface may be valid for some metals (*e.g.*, Cu and Pb), and, indeed, has been shown to be workable (see, for example, references 21 and 25). However, data presented here for Au and Ag suggest that atoms which re-desorb from secondary sites do so with $E_a$ values substantially different from their primary-site counterparts. This fact may serve to explain the relatively poor fit between the experimental and calculated source functions obtained by van den Broek and de Galan[3] for Ag and Mn and their success with Pb. These data should prove useful for application in Monte Carlo modelling techniques.[22]

Although it is tempting to correlate $E_a$ values for secondary-site desorption with analyte - graphite interaction energies,

this approach overlooks the possibility of atoms preferentially adsorbing on to impurities on the tube surface (*i.e.*, chemisorbed oxygen) rather than on the graphite substrate itself.[21]

Financial support for S. L. by the Ministry of Agriculture, Fisheries and Food is gratefully acknowledged. We thank B. Hutsch (Ringsdorff-Werke, FRG) for kindly supplying the glassy carbon and pyrolytic graphite coated T-tubes and D. Downham for the transmission electron micrograph work.

## References

1. Holcombe, J. A., and Rayson, G. D., *Prog. Anal. At. Spectrosc.*, 1983, **6**, 225.
2. L'vov, B. V., Nikolaev, V. G., Novichikhin, A. V., and Polzik, L. K., *Spectrochim. Acta, Part B*, 1988, **43**, 1141.
3. van den Broek, W. M. G. T., and de Galan, L., *Anal. Chem.*, 1977, **49**, 2176.
4. Schlemmer, G., and Welz, B., *Fresenius Z. Anal. Chem.*, 1986, **323**, 703.
5. Holcombe, J. A., Rayson, G. D., and Akerlind, N., Jr., *Spectrochim. Acta, Part B*, 1982, **37**, 319.
6. Paveri Fontana, S. L., Tessari, G., and Torsi, G., *Anal. Chem.*, 1974, **46**, 1032.
7. Paveri Fontana, S. L., Tessari, G., and Torsi, G., *Ann. Chim. (Rome)*, 1979, **69**, 943.
8. Musil, J., and Rubeška, I., *Analyst*, 1982, **107**, 588.
9. Welz, B., Radziuk, B., and Schlemmer, G., *Spectrochim. Acta, Part B*, 1988, **43**, 749.
10. Grinshtein, I. L., Vasil'eva, L. A., and Katskov, D. A., *Zh. Prikl. Spektrosk.*, 1987, **46**, 13.
11. McNally, J., and Holcombe, J. A., *Anal. Chem.*, 1987, **59**, 1105.
12. Holcombe, J. A., personal communication, 1989.
13. Smets, B., *Spectrochim. Acta, Part B*, 1984, **35**, 33.
14. Falk, H., *Spectrochim. Acta, Part B*, 1984, **39**, 387.
15. Manning, D. C., and Ediger, R. D., *At. Absorpt. Newsl.*, 1976, **15**, 42.
16. Slavin, W., and Manning, D. C., *Spectrochim. Acta, Part B*, 1982, **37**, 955.
17. Holcombe, J. A., and Droessler, M. S., *Fresenius Z. Anal. Chem.*, 1986, **323**, 689.
18. Sturgeon, R. E., and Arlow, J. S., *J. Anal. At. Spectrom.*, 1986, **1**, 359.
19. Sturgeon, R. E., and Berman, S. S., *Anal. Chem.*, 1985, **57**, 1268.
20. Bass, D. A., and Holcombe, J. A., *Anal. Chem.*, 1988, **60**, 578.
21. Baird, T., Fryer, J. R., Arbuthnott, A. R., McAneney, B., Riddell, E. V., and Walker, D., *Carbon*, 1974, **12**, 381.
22. Black, S. S., Riddle, M. R., and Holcombe, J. A., *Appl. Spectrosc.*, 1986, **40**, 925.
23. Wang, P., Majidi, V., and Holcombe, J. A., *Anal. Chem.*, 1989, **61**, 2652.
24. Arthur, J. R., and Cho, A. Y., *Surf. Sci.*, 1973, **36**, 641.
25. Guerrieri, A., Lampugnani, L., and Tessari, G., *Spectrochim. Acta, Part B*, 1984, **39**, 193.

*Paper 9/05146E*
*Received November 28th, 1989*
*Accepted February 20th, 1990*